JTTEE5 19:178–189
DOI: 10.1007/s11666-009-9361-y
1059-9630/$19.00 © ASM International

Peer Reviewed

Characterization of Complex Thermal Barrier Deposits Pore Microstructures by a Combination of Imaging, Scattering, and Intrusion Techniques

J. Ilavsky

(Submitted March 30, 2009; in revised form June 5, 2009)

Complexity, wide size ranges, and anisotropy are attributes that can describe porous microstructures of thermally sprayed deposits, which present especially difficult challenges for characterization techniques. A number of different methods have been utilized and found to be useful while having significant limitations. Therefore, scientists and engineers need to understand the advantages, limitations, and disadvantages of each technique. This very short review attempts to present a wide range of characterization tools—from frequently employed optical and scanning electron imaging techniques, through intrusion porosimetry, to lesser-used x-ray and neutron imaging and scattering techniques. It will be shown that no technique in itself is sufficient and that a properly selected combination of techniques is necessary to get a sufficiently complex characterization method. A really powerful and capable characterization protocol may need to combine fast and accessible ("in-house") tools with sparingly applied advanced scattering and imaging techniques. Such a combination of techniques can then be utilized to research the processing-microstructure-properties relationships as well as to provide sufficient data for development of successful models.

Keywords imaging techniques, intrusion porosimetry, microstructure characterization, porosity, small-angle scattering

1. Introduction

Thermal barrier deposits (TBCs) for high-heat-load engines such as aircraft or land-based turbines (Ref 1) are usually either thermally sprayed (TS) or electron-beam physically vapor deposited (EBPVD) (Ref 2, 3). They commonly contain porosity-a term for voids in the material-either unwanted, as a result of an imperfect manufacturing process, or desired, i.e., functional, possibly painstakingly designed (Ref 4). The void system design has a potential to be the path to improve engineering properties of current and future materials, e.g., reduced weight, increased life, and improved efficiency and safety. Multiple functions of the voids need to be balanced, e.g., reduction of the thermal conductivity of the material and increased compliance of the material to stresses caused by in-service thermal expansion and contraction during thermal cycles and other stress-generating processes (Ref 5). As the operating temperatures of the turbines are increasing to improve the efficiency, combustion chamber temperatures increase, and improved materials are needed (Ref 6). By mid-1990s, the limits of metallic materials had been reached (Fig. 1), but application of TBCs (Fig. 2) allowed operating temperatures to increase to today's nearly 1300 °C. Commonly used ceramic yttria-stabilized zirconia (Zr_2O_3 + about 8% Y_2O_3 by mass) TBCs protect the underlying metal against the high combustion temperatures. Furthermore, they can provide some improved level of corrosion protection.

Ceramic TBCs are complicated engineering material systems manufactured by a number of competing technologies (Ref 6-9). Each method produces very different coating microstructures (Ref 10). And since they all are versatile processes (Ref 11, 12), materials engineers do have a lot of flexibility in designing the microstructure that best fit a particular application.

2. Porosity Characterization

The optimization of a material for any specific application includes a number of steps, such as understanding

This article is an invited paper selected from presentations at the 2009 International Thermal Spray Conference and has been expanded from the original presentation. It is simultaneously published in *Expanding Thermal Spray Performance to New Markets and Applications: Proceedings of the 2009 International Thermal Spray Conference*, Las Vegas, Nevada, USA, May 4-7, 2009, Basil R. Marple, Margaret M. Hyland, Yuk-Chiu Lau, Chang-Jiu Li, Rogerio S. Lima, and Ghislain Montavon, Ed., ASM International, Materials Park, OH, 2009.

J. Ilavsky, Advanced Photon Source, Argonne National Laboratory, Argonne, IL. Contact e-mail: ilavsky@aps.anl.gov.

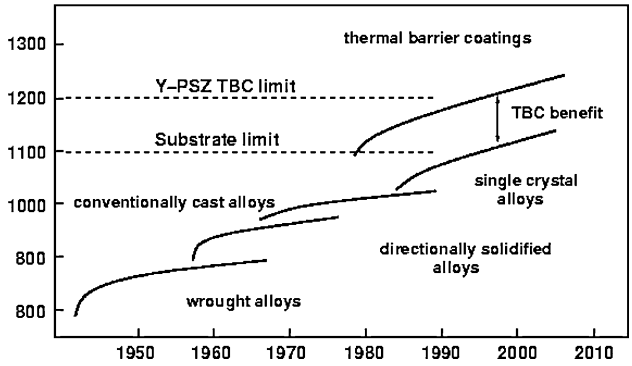

Fig. 1 Trend of the inlet temperatures according to the employed alloys and the benefit of the usage of TBCs (Ref 1)

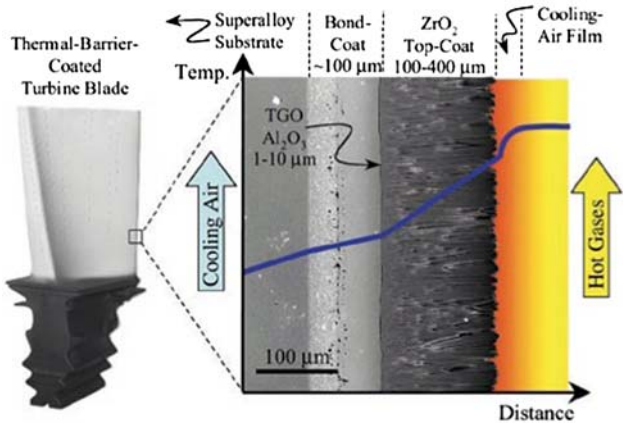

Fig. 2 Structure of typical EBPVD TBC system in gas turbine engines (Ref 3). Blue curve indicates in-service temperature

the operational environment, the materials requirements, and materials availability and performance. In the design of a porous microstructure for a specific application, the underlying assumption is that we can

1. characterize the microstructure/porosity,
2. control and modify the porous microstructure, and
3. understand the relationship between the microstructure and engineering properties.

The first item on this list is the target of this review; the second item is a subject that, with varying levels of complexity, has been studied and is discussed in references listed here. Several examples of reviews of porosity relationships with engineering properties, such as elastic properties (Ref 13, 14) or thermal conductivity (Ref 15, 16), can be found.

The pore characterization may be challenging (Ref 17) and, for many techniques, problematic to address as the pores may exhibit some or all of the following specific characteristics:

1. wide size range—generally in the range of 1 nm to over 10 µm
2. pore system anisotropy
3. complex or limited pore connectivity
4. complicated pore shapes
5. opaque to visible light

2.1 Porosity Descriptors

One of the important questions is: What description of the pore microstructure is appropriate and sufficient for the needs of engineers and scientists? Following are some potential candidates that are or usually should be considered.

- *Porosity (pore volume)* as a fraction of the overall sample volume is the most commonly used descriptor of the pore microstructure.
- *Pore size distribution.* Large pores or small pores? Which are better? That depends on the applications and material. Most manufacturing processes result in a wide range of void sizes rather than a single size. Establishing the extent of sizes and distribution of pores can be of major importance in understanding a material's properties.
- *Pore shapes.* Often the pores in the material are modeled as spherical voids, nicely separated from each other. Unfortunately, this simple model, for the majority of engineering materials, is simply wrong. For more complicated pore microstructures, one can imagine pores that are better approximated by other geometrical shapes, such as ellipsoids or platelets.
- *Pore connectivity.* Are the pores connected or isolated? What fraction of pores can be accessed from the surface?
- *Pore surface area.* Surface area of pores—expressed as specific surface area per volume of weight or volume of sample.
- *Pore anisotropy.* The anisotropy of the void system can be of major importance especially for highly anisotropic microstructures.

3. Techniques

The following is a simplified grouping of the techniques reviewed here:

- 2D imaging techniques using visible light or other probes (e.g., electron beams) combined with stereology methods.
- 2D imaging-based tomography using a series of 2D images of opaque samples to reconstruct the 3D structure of materials.
- Intrusion techniques by filling the voids within the sample with filler material.

- 3D imaging techniques and tomography methods using a probe that penetrates the sample volume—like x-rays or neutrons—to create an image based on absorption or phase contrast.
- Small-angle scattering (SAS) techniques using scattering of x-rays or neutrons while passing through the sample.

In general, there is no ideal single technique that one could choose to get the necessary descriptors of the pore system. Each of these techniques has advantages and disadvantages (Ref 18, 19). Selection of an optimal technique, or set of techniques, is contingent upon an understanding of the limitations and capabilities of each.

3.1 2D Imaging Techniques and Stereology

Two-dimensional imaging techniques are the most common methods used to study the structure of materials. They share the same strategy—selected representative surface of an opaque sample is imaged by a suitable method. This image is then processed (manually or with the help of computers) to extract information about the internal structure. An informal review of selected publications in the thermal spray field (using proceedings of the International Thermal Spray Conference) shows that about 90% of publications that deal with the microstructure of the materials include optical or some other type of microscopy.

In these methods, the preparation of the representative sample surfaces is probably the critical factor influencing results of the study. The two major types of surfaces studied are fracture surfaces and polished cross sections, and accepted practice methods were developed for sample preparation (Ref 20-22).

Many types of 2D imaging instruments are available—from optical microscopes (OM), scanning electron microscopes (SEM), and transmission electron microscopes (TEM) to atomic force microscopy (AFM) and other tools. All of these techniques result in a 2D representation of the surface of the sample with some contrast mechanism, which can be color, surface profile, chemical composition, etc. These images are then processed and microstructure descriptors are obtained by stereology methods (Ref 23-26). Even with an ideally prepared sample surface, stereology is limited by the resolution limit of the techniques used for imaging and the fact that only 2D information is available (Ref 27, 28). An understanding of meaningful resolution limit is very important for the study of microstructures with wide ranges of void sizes. Limited improvement can be obtained, for example, by increasing the number of images collected on a sample (Ref 29).

Measurement of pore anisotropy in the most general case is challenging. Fortunately, many of the coating microstructures exhibit one isotropic direction (Ref 30). If this isotropic direction is known, even anisotropic microstructures can be characterized reasonably well by studying the cross sections in the plane parallel to the isotropic direction (Ref 31, 32).

3.2 2D Imaging-Based 3D Tomography

Recently, real 3D reconstructions using multiple 2D images became common. These 3D reconstructions can be achieved through various methods—mechanical layer removal combined with optical microscopy (Fig. 3) (Ref 29, 33) or focus-ion-beam milling combined with SEM (Fig. 4) (Ref 34). These methods can be time consuming but yield the real 3D microstructure of the material using commonly available tools.

3.3 Intrusion Porosimetry

Intrusion porosimetry techniques fill the voids in the material with selected probe material: either gas (typically helium or nitrogen) or a liquid (mercury or water). The volume of probe material is measured, potentially as a

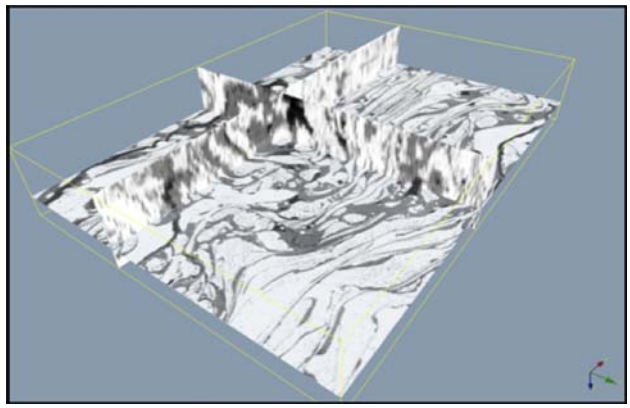

Fig. 3 3D reconstruction of thermally sprayed steel coating. Metal is white, oxides are gray, and pores are black (Ref 33)

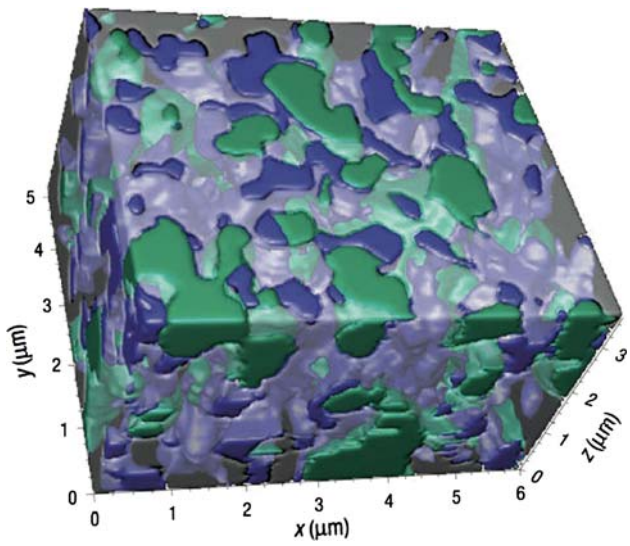

Fig. 4 3D reconstruction of YSZ anode of solid-oxide fuel cell system. This 3D map of materials now can be processed to obtain 3D distribution of important features (like triple phase boundaries) (Ref 34)

function of filling pressure. Characteristics of the void system are deduced from the pressure dependence based on the model (Ref 35). For complex TBC microstructures, intrusion porosimetry can be a very useful technique for measuring total porosity volume in samples, which can be obtained in sufficient amounts and are not reactive with mercury or the intruding medium. The pore size and specific surface area distributions from intrusion porosimetry are due to model assumptions not reality, and there is, basically, no way to address the voids' anisotropy. Also, different populations of voids present in a sample can be distinguished only if they differ significantly in size.

3.4 X-Ray and Neutron Techniques

An increasing availability of high-flux (synchrotron) x-ray sources, high-performance desktop x-ray instruments, and reactors and spallation sources for neutrons has enabled development of techniques for microstructure characterization of materials using these probes. These techniques can be broadly divided in two basic categories—imaging and scattering techniques. In both of these categories, the beam of x-ray or neutron radiation is passed through the sample while being subjected to both absorption (or phase shift) and scattering.

Absorption—or sometimes phase contrast—is utilized by imaging techniques. The beam is passed through the sample, and the beam modified by absorption and/or phase contrast is captured on a point (0D), line (1D), or area (2D) detector with or without x-ray magnification. In tomography, a series of images (usually using absorption contrast) is reconstructed using computer programs to create a 3D volumetric map of density inside the sample (Ref 36).

In scattering techniques, the beam passes through the sample and scatters on the interfaces within the sample. The scattered intensity is measured as a function of scattering angle and is used to provide information about the microstructure. Since the scattering provides information in the Fourier space, reconstruction of the microstructure from scattering data usually requires a model approach. Some information, however, can be obtained without models.

X-ray and neutron techniques share common features of importance for porosity measurements of complex materials:

- Voids do not have to be accessible from the outside of the sample (i.e., opened) to be measured.
- Materials and radiation selection is important, as absorption and scattering properties vary for different materials and radiation types.

3.4.1 Small-Angle Scattering Techniques. A wide range of techniques was developed for materials characterization using small-angle scattering (SAS), varying in instrumentation and/or methods used. Most common small-angle x-ray scattering (SAXS) and small-angle neutron scattering (SANS) techniques probe microstructural features in sizes from about 1 nm up to approximately 100 nm (Ref 37). Ultra small-angle x-ray scattering (USAXS) and neutron scattering (USANS) techniques and instrumentations were developed, which extend this range up to 10 μm (Ref 38).

Small-angle scattering is caused by differences in x-ray or neutron contrasts within the sample—in the case of voids, between the solid phases and air. The x-ray contrast is proportional to the density of the electrons in the material, which, with reasonable precision, is related to the material density (Ref 39).

3.4.2 Anisotropic Small-Angle Scattering (Dilute Limit). For material systems that can be approximated as a population of spheroidal shape scatterers, an analytic formula has been developed (Ref 40). A microstructural model, based on this formula, composed of up to six populations was used (Ref 41). Here, the microstructure of the plasma-sprayed thermal barrier deposits was considered to contain three populations of voids—interlamellar pores of aspect ratio 0.2, intralamellar cracks of aspect ratio 0.1, and spherical voids, based on SEM images (Fig. 5). By using this model and data from a USAXS instrument, quantitative volumes for the different populations of voids were obtained.

The complex microstructure of EBPVD coatings was quantitatively characterized by Flores-Renteria et al. (Ref 1, 42, 43) and Dobbins et al. (Ref 44). In both of these cases, the USAXS instrument was used to collect data in specially prepared samples in cross section. Using a model described in Ref 41, these authors were able to take advantage of the different anisotropies, shapes, and sizes of the void populations (Fig. 6) and obtain full characterization of this complex void system, i.e., they were able to assign (model based) opening dimensions, shapes, anisotropies, and volumes to each of the populations of voids. The coatings were studied both as-deposited and annealed, simulating in-service conditions. The thermal conductivity of these microstructures, as predicted by

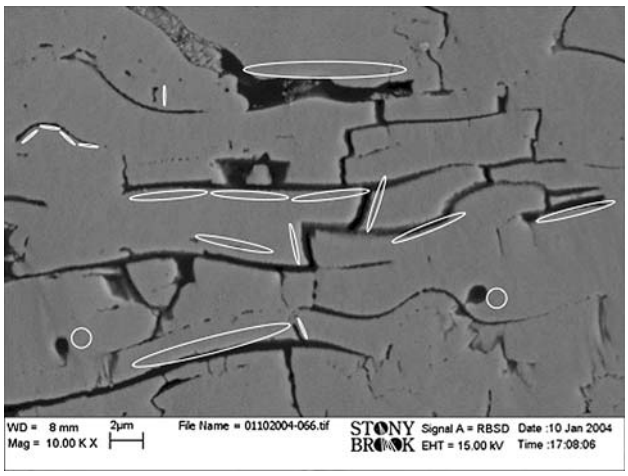

Fig. 5 Microstructure with selected examples of model shapes next to voids. The ellipses represent cross-section profiles of the model spherical voids or oblate ellipsoidal voids with aspect ratio 1/10 (Ref 41)

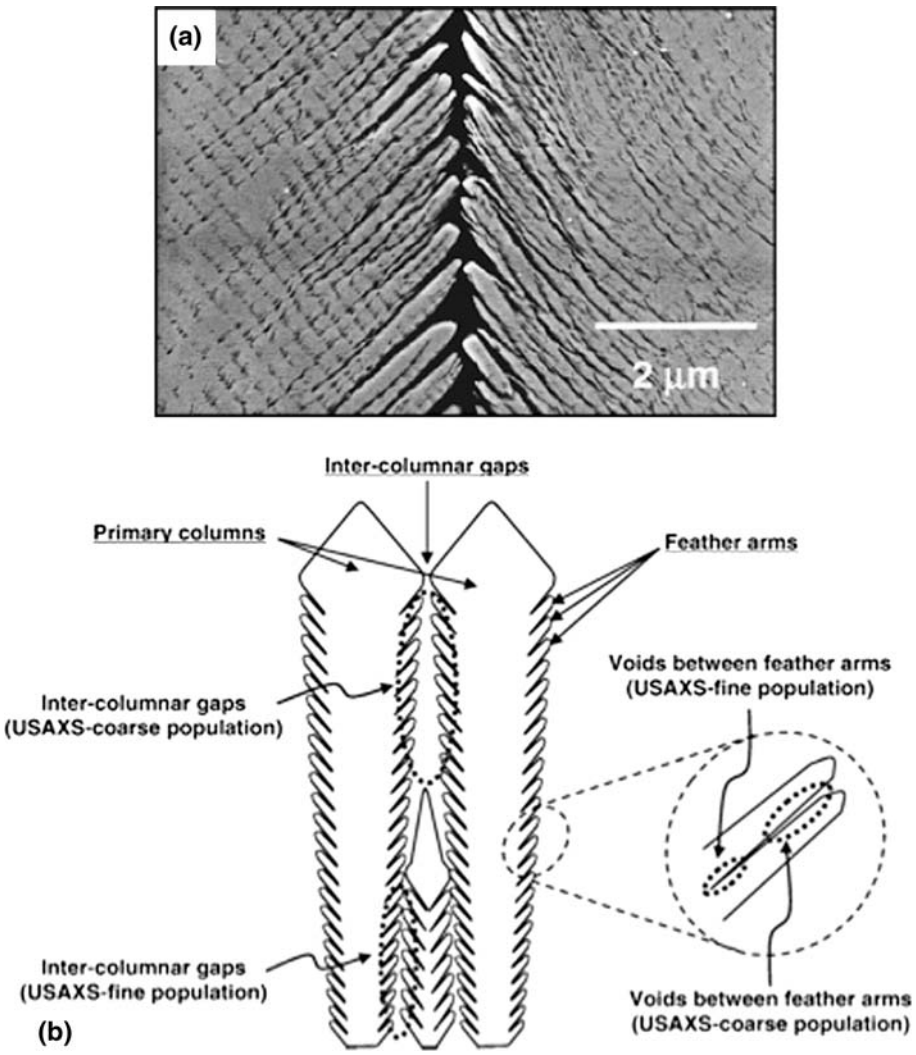

Fig. 6 SEM micrograph (a) of as-deposited EB-PVD manufactured YSZ TBC coatings. Schematics of model assumptions (b) for USAXS data analysis. The microstructure model in this case contained four populations: intercolumnar gaps coarse and fine and feather-like pores coarse and fine (Ref 1)

semi-empirical approximation (Ref 45), was calculated and found to be in good agreement with the results of measurements.

3.4.3 Anisotropic Porod Scattering. Anisotropic Porod scattering has proven to be a particularly useful tool for discerning changes of the smallest void systems, which usually cannot be characterized by other techniques. The characterization is based on both the absolute value of specific surface area as well as changes in the measured anisotropy, as deduced from the anisotropy of the apparent Porod surface distribution (Fig. 7). The first studies using this technique concentrated on microstructure variations, due to feedstock characteristics (Ref 32, 46) (e.g., chemistry, manufacturing method, feedstock size), and simulated in-service conditions of thermal barrier coatings (see Fig. 8) (Ref 47). For example, a detailed analysis of spray angle effects on the coating microstructure has been studied by Ilavsky et al. (Ref 48). The two main anisotropic void systems—interlamellar pores and intralamellar cracks—were found to behave differently with deviation of spray angle from the normal direction. The interlamellar pores stayed preferentially parallel with the substrate, whereas the intralamellar crack system tilted partially as the spray angle changed (Fig. 9). Using mercury intrusion porosimetry, authors observed a near tripling of the porosity with a decrease of the spray angle to 30°. The effect of the spray angle on mechanical properties was later studied (Ref 49).

In later experiments, the open pores in the plasma-sprayed alumina deposits were filled (using vacuum impregnation) with a mixture of H_2O and D_2O (Ref 50) with composition tailored to contrast match the alumina for neutrons. Then the measured data were only from voids that were closed under these conditions. In combination with mercury and water intrusion techniques, this work concluded that while most of the pore volume is in

large and open voids, more than 60% of the total specific surface area of voids is actually in the closed pores, which could not be intruded.

Using this method, it is possible to independently characterize the major anisotropic void systems in the coatings and study their changes with spray conditions or postprocessing (Ref 46, 51). An in situ SANS experiment (Ref 52) with YSZ TBC materials quantified the microstructural changes as the temperature was increasing at a rate of 50 °C per hour from 600 to 1400 °C. The two main anisotropic void systems were quantified (Fig. 10). By the time the sample reached about 1000 °C, the total pore-specific surface area was reduced by about 1/3 due to sintering, and virtually all of these losses occurred in the fine crack system, which basically disappeared. Above 1000 °C, the sintering continued, resulting in reduction of the interlamellar pores.

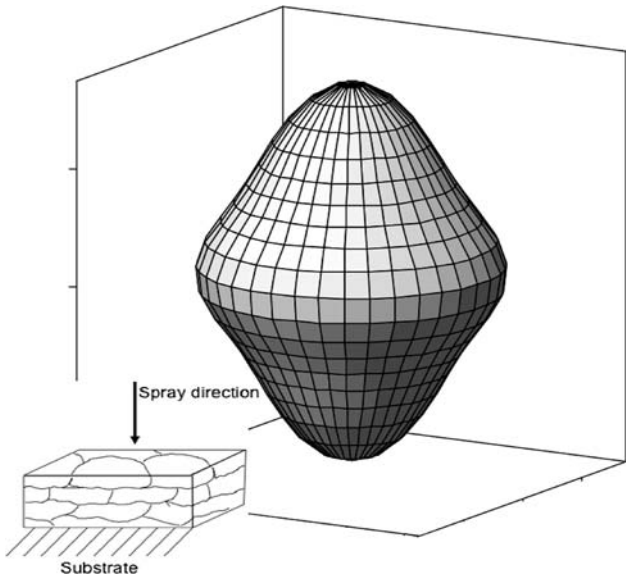

Fig. 7 Measured 3D anisotropy of the apparent Porod-specific surface for plasma-sprayed YSZ. Drawing indicates orientation of the deposits with respect to the orientation of the axis (Ref 30)

3.4.4 Multiple Small-Angle Scattering (MSAS). In many engineering materials (e.g., ceramics, coatings), SAS is frequently dominated by a ''multiple scattering'' situation when the probability of the scattering of each photon or neutron is higher than one as it passes through the sample. For anisotropic engineering materials, the theory of multiple scattering was developed (Ref 53) and applied to study TBC systems (Ref 54, 55). Typically, the microstructure was modeled as a three-component system with a population of interlamellar pores, intralamellar cracks, and spherical pores (Ref 40).

This technique was extensively applied to studies of the influence of feedstock, spray conditions, and postprocessing (annealing) on ceramic coatings (Ref 52) or metallic coatings (Ref 56-58). The results were combined with other porosity characterization methods to provide a broader picture of the microstructure (Ref 59-61). Figure 11 shows an example of the unique results one can obtain by applying the MSAS technique to an appropriate problem. In this case, microstructural changes related to annealing at various temperatures were studied, and the application of MSAS combined with other techniques enabled independent characterization of the components in the microstructure (Ref 40).

3.5 3D Imaging Techniques (Tomography)

3.5.1 X-Ray Microtomography. X-ray microtomography in materials science is well documented in its ''non-magnified'' variation, when no magnification of x-rays is performed (Ref 36). Due to the limitations of x-ray detectors, the resolution limit is about 1 μm. Unless a major breakthrough in detection is achieved, it will not significantly improve. During measurement, the x-ray beam passes through the sample and multiple images are

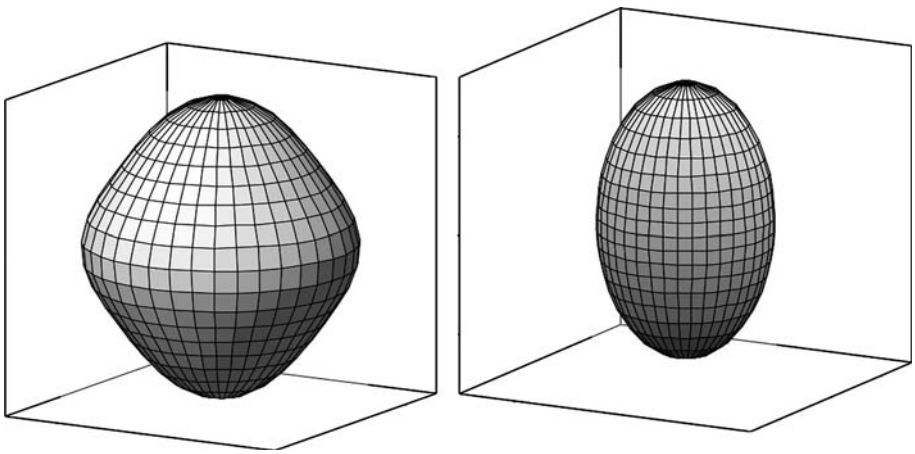

Fig. 8 Change in apparent Porod anisotropy during simulated in-service conditions. As deposited (left) and after 1200 °C for 1 h annealing (right) (Ref 47). Change in anisotropy indicates preferential sintering of crack void system

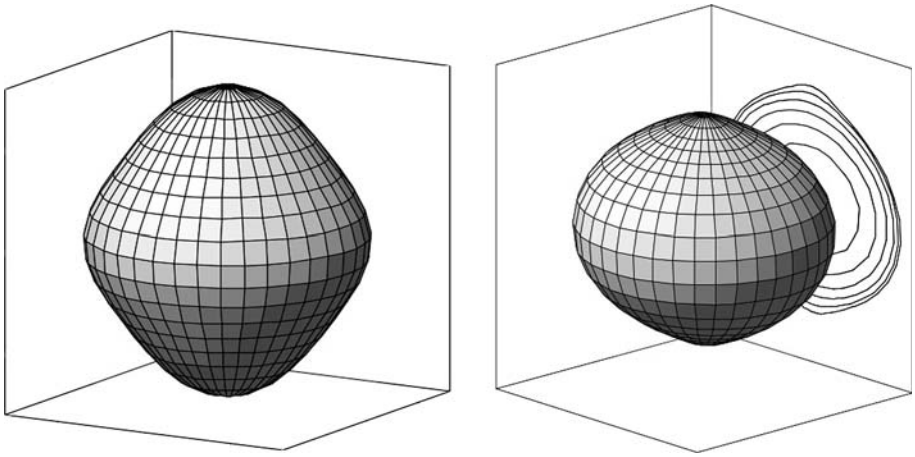

Fig. 9 Apparent Porod surface-area distribution for samples sprayed at a spray angle 90° (left) and 50° (right). The 50° results can be decomposed into interlamellar pore system, which does not change with spray angle (is parallel with substrate), and crack system, which orientation follows the spray angle (Ref 48)

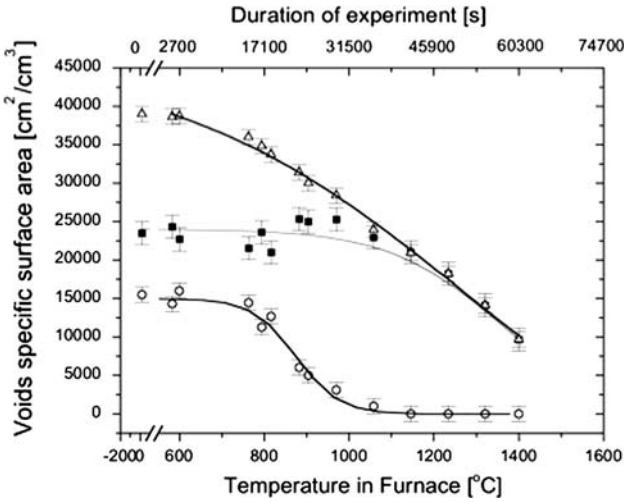

Fig. 10 Quantitative changes of specific Porod surface areas in thermally sprayed YSZ during annealing. Open triangles: total pore specific surface area; closed squares: interlamellar pores' specific surface area; and open circles: cracks' specific surface area (Ref 81)

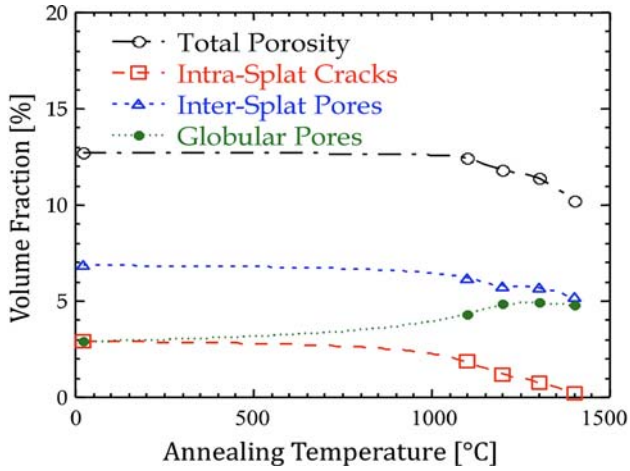

Fig. 11 Multiple small-angle scattering-derived total and component void porosities vs. 1 h annealing temperature for plasma-sprayed YSZ thermal barrier coatings (Ref 40)

recorded as the sample is rotated. These are processed using various algorithms to obtain a 3D density map distribution (Ref 62). Neutrons can be also used for tomography (Ref 63), though with limited resolution. Advances in neutron sources (e.g., Spallation Neutron Source (Ref 64)) and detection techniques may make this technique feasible in the future.

3.5.2 Magnified Tomography. Magnified tomography techniques use magnification of the x-ray beam after it passes through the sample and before conversion to visible light. The resolution is then given by a combination of the detector resolution and overall magnification of the x-ray image, resulting in potentially 30 nm or better resolution. Magnification by asymmetric Bragg reflection (Ref 65-67) improves the resolution to about 100 nm but with a large and well-illuminated field of view. Further improvements in spatial resolution of x-ray tomography were lately enabled by developments in optical elements for hard x-rays that perform similar to lenses for visible light and make x-ray microscopes possible. These instruments are just becoming available for application on complex engineering materials.

3.6 Combination of Techniques

Kulkarni et al. published a number of studies on thermally sprayed and EBPVD TBC materials in which they combined many techniques, including SAS techniques and nonmagnified tomography (Ref 61, 68-73). The 2006 paper on EBPVD deposits (Ref 68) combines SANS (Porod surface anisotropy and multiple SANS (MSANS) techniques), SAXS, and tomography to document how full quantitative characterization of this complex microstructure,

including anisotropy and variation through thickness, can be obtained. Previously (Ref 61, 69), authors addressed similar plasma-sprayed TBC or high-velocity oxygen fuel-sprayed (Ref 60) deposits. By combining SANS and imaging techniques with intrusion and SEM/OM imaging, they were able to relate the microstructure parameters to measured engineering properties such as thermal conductivity or elastic modulus. They have shown that, in general, very good agreement can be obtained between measured and calculated properties if the microstructure description is sufficiently detailed and complex.

Studies have compared the widely available imaging techniques with SAS (Ref 30) or SAS and tomography (Ref 74) to document the limits of applicability of the imaging techniques. In summary, properly implemented imaging techniques, when combined with proper sample preparation, were confirmed (within resolution limits) to be quite suitable to address specific aspects of the microstructure, such as anisotropy. The imaging results may not be reliably quantitative though, due to resolution limits and other issues. Where the imaging techniques excel is in comparison of large numbers of samples and identification of differences between them.

4. Other Types of Coatings

This review concentrates on thermal barrier coating microstructures, with additional examples from other areas of complex engineering materials, such as solid-oxide fuel cells. A large number of the publications have been in this area, but there are many more materials with complex voids microstructures, both thermal sprayed and manufactured by other methods. All the issues discussed here are fully applicable to other microstructures, with the specifics of those microstructures. Two examples of such microstructures are discussed below, though with fewer references, as some of these results are based on ongoing current research that has not been published yet.

Suspension plasma spray (SPS) and solution precursor plasma spray (SPPS) coatings (Ref 75, 76) are two microstructures with promising futures. In preliminary experiments on these materials, we have observed unique microstructural features that pose specific challenges. These coatings are formed by submicron-sized particles, and the voids are similarly small. Therefore, these microstructures are really challenging for most imaging techniques. These materials can be manufactured in a wide range of porosity volumes, specific surface areas, and thicknesses. Polishing of high-porosity samples can be a major source of errors and uncertainties for imaging techniques. Intrusion porosimetry is a very valuable technique for samples with sufficient overall volume, but may be of limited value for thin and small-volume samples.

Preliminary results using various SAS techniques were obtained on two very different types of coatings—high-porosity coatings for potential application as thermal barrier coatings (Ref 77) and low-porosity thin layers for solid-oxide fuel cell structures. These materials were found to exhibit practically isotropic microstructures, as observed using anisotropic Porod scattering. Using dilute limit SAS, applicable in at least in some cases, we observed void structures, which were clearly limited to sizes less than 1 μm. Future research should provide more insight into these materials, but these preliminary results show that these materials will be challenging the resolution limits of most imaging techniques.

Vacuum plasma-sprayed (VPS) (Ref 78) and high-velocity oxy fuel (HVOF) (Ref 12)-sprayed coatings are two other challenging types of microstructures. They are often low-porosity materials (below 2%) and are often made from metals or ceramic-metal composites. The limitations faced by various techniques are, again, related to the specifics of these microstructures. For example, for intrusion porosimetry, the level of connectivity among the low volume of voids should not be anticipated; this can result in an underestimation of the real porosity. Also, some metals have potential for reacting with mercury. Polishing of metallic coatings also can be challenging due to metallic material smearing (Ref 79), which would also reduce the amount of porosity observed. Small-angle scattering and tomography are good techniques, yet there may be issues with small-angle neutron scattering on magnetic materials. For x-rays, there are issues with high absorption of higher density metals, which can result in the need for very thin samples. Limited research on using a combination of small-angle techniques, imaging, and intrusion techniques is available in the literature (Ref 80).

5. Conclusions

A number of methods suitable for pore microstructure characterization of thermally sprayed deposits and other complex engineering materials are available, each with specific limitations, see Table 1. Generally, no single technique is sufficient alone, and a combination of techniques may need to be applied depending on the descriptor or descriptors needed, see Table 2. It should be recognized that the most effective approach is to properly select one or few methods after careful consideration of the needs of a given problem. While tomography or SAS techniques may not be readily accessible or may require a long lead time before an experiment can be performed, they should become a part of one's generally used technique portfolio. An optimized approach to microstructure characterization may be to combine various techniques together, similar to the following:

1. Use imaging and intrusion techniques to identify the range of microstructures to be studied, finding both the representative and outlying samples.
2. Perform a combination of experiments (SAS or tomography) to characterize a limited number of microstructures to obtain a model and understand the important microstructural features.

Table 1 Summary of capabilities of various porosity characterization techniques

Technique	Minimum size, nm	Maximum size, μm	3D distribution or model	Porosity volume	Pore size distribution	Pore shapes	Pore connectivity	Pore anisotropy	Pore surface area	Main limitations
Optical microscopy (OM)	300	···	···	Yes	Yes	Yes	No	Yes	Limited	Resolution, sample preparation
Scanning electron microscopy (SEM)	~5	···	···	Yes	Yes	Yes	No	Yes	Limited	Sample preparation
3D Tomography using 2D techniques	Varies	···	3D distribution	Yes	Yes	Yes	Yes	Yes	Yes	Labor intensive
Transmission electron microscopy (TEM)	0.1-1	100-1000	···	No	No	Yes	No	No	No	Very small volume, preparation
Mercury intrusion porosimetry (MIP)	10	100	···	Yes	Limited by model	No	Limited(a)	No	Yes (open)	Model based, sample volume large
Gas adsorption	0.1	···	···	Yes	No	No	Limited(a)	No	Yes (open)	Sample volume large
Archimedean porosimetry	Varies	Varies	···	Yes	No	No	Limited(a)	No	No	Sample volume large
Multiple small-angle scattering	100	5	Model	Yes	No	Model	No	Yes	No	Limited applicability
Anisotropic-specific surface area	1	~5	···	No	No	Partial	No	Yes	Yes	···
Anisotropic single SAS	1	~5	Model	Yes	Yes	Yes	No	Yes	Yes	···
X-ray microtomography	1000	Varies	3D distribution	Yes	Yes	Yes	Yes	Yes	Yes	Resolution limited
X-ray magnified tomography	10	0.1	3D distribution	Yes	Yes	Yes	Yes	Yes	Yes	Small field of view

(a) Can quantify open/closed

Table 2 Selected descriptors of void structure and appropriate choices of characterization tools

Void system descriptor	Most appropriate techniques	Other good choices	Comment
Porosity (volume)	Intrusion porosimetry	Many other techniques	Limitations of techniques vary
Size distribution	Tomography, small-angle scattering	2D imaging, intrusion porosimetry	Size range for techniques varies
Shapes	Tomography	2D imaging	...
Connectivity	Tomography	Intrusion technique	Size range for tomography
Specific surface area	Small-angle scattering, intrusion porosimetry	Tomography	Intrusion is model based, limited size range for tomography
Anisotropy	Tomography	2D imaging, small-angle scattering	...

3. Perform analyses using various modeling methods to identify the microstructural features that are influential in the experiment, and are therefore necessary to quantify, in order to develop a process or understand the properties. Specifically, it is important to properly judge the size range of the pores of interest, their morphology, and accessibility.
4. Select the most effective characterization method for characterization of the whole experimental sample set. The analysis method for these measurements can be guided by the model available from step 2 above.

By using this approach, reliable and robust microstructure data will be used, and the experiment will be effective.

Acknowledgment

This work was supported by U.S. Department of Energy, Office of Science, Office of Basic Energy Sciences under contract No. DE-AC02-06CH11357.

References

1. A.F. Renteria, "Small-Angle Scattering Analysis of the Manufacture and Thermal Induced Morphological Changes and Their Influence in the Thermal Conductivity of EB-PVD PYSZ TBCs," Ph.D. Thesis, Rheinish-Westfalischen Technischen Hochshulle Aachen, RWTH Aachen University, 2007
2. H. Brill-Edwards, Historical Evolution on EB-PVD Thermal Barrier Coatings in Aero and Industrial Gas Turbines, *Proc. Technology Symposium on High Temperature Gas Turbine Coatings*, ITA, Dresden 1998
3. N.P. Padture, M. Gell, and E.H. Jordan, Materials Science—Thermal Barrier Coatings for Gas-Turbine Engine Applications, *Science*, 2002, **296**(5566), p 280-284
4. A. Weber and E. Ivers-Tiffee, Materials and Concepts for Solid Oxide Fuel Cells (SOFCs) in Stationary and Mobile Applications, *J. Power Sources*, 2004, **127**(1-2), p 273-283
5. H. Guo, H. Murakami, and S. Kuroda, Effects of Heat Treatment on Microstructures and Physical Properties of Segmented Thermal Barrier Coatings, *Mater. Trans.*, 2005, **46**(8), p 1775-1778
6. M.R. Dorfman, M. Nonni, J. Mallon, W. Woodard, and P. Meyer, Thermal Spray Technology Growth in Gas Turbine Coatings, *ITSC 2004 Thermal Spray Solutions—Advances in Technology and Applications, Proceedings of the International Thermal Spray Conference*, 10-12 May, 2004 (Osaka, Japan), ASM International, Materials Park, OH, 2004, p 1-6
7. D.R. Clarke and S.R. Phillpot, Thermal Barrier Coating Materials, *Mater. Today*, 2005, **8**(6), p 22-29
8. M.R. Dorfman, C. Dambra, and J. Wallon, Hotter than Ever: Coatings Improve Turbine Performance, *Sulzer Tech. Rev.*, 2004, **86**(2), p 14-16
9. Q. Du, X. Liu, J. Guo, and Q.-C. Sun, Thermal Barrier Coating-Thermal Conductivity Measurement Methods to Reduce the Thermal Conductivity, *Gongneng Cailiao/J. Funct. Mater.*, 2005, **36**(7), p 1100-1106
10. R.C. Tucker, Jr., An Overview of Thermal Spray Coatings Compared to Physical and Chemical Vapor Deposited Coatings, *14th International Thermal Spray Conference: Thermal Spraying-Current Status and Future Trends*, A. Ohmori, Ed. (Kobe, Japan), High Temperature Society of Japan, 1995, p 253-258
11. P. Fauchais, M. Fukumoto, A. Vardelle, and M. Vardelle, Knowledge Concerning Splat Formation: An Invited Review, *J. Therm. Spray Technol.*, 2004, **13**(3), p 337-360
12. P. Fauchais, A. Vardelle, and B. Dussoubs, Quo Vadis Thermal Spraying?, *J. Therm. Spray Technol.*, 2001, **10**(1), p 44-66
13. M. Ashizuka, E. Ishida, T. Matsushita, and M. Hisanaga, Elastic Modulus, Strength and Fracture Toughness of Alumina Ceramics Containing Pores, *J. Ceram. Soc. Jpn*, 2002, **110**(6), p 554-559
14. M. Kaczmarek and M. Goueygou, Dependence of Elastic Properties of Materials on Their Porosity: Review of Models, *J. Porous Media*, 2006, **9**(4), p 335-355
15. L. Braginsky, V. Shklover, G. Witz, and H.P. Bossmann, Thermal Conductivity of Porous Structures, *Phys. Rev. B*, 2007, **75**(9), p 10
16. M.R. Wang, J.K. Wang, N. Pan, and S.Y. Chen, Mesoscopic Predictions of the Effective Thermal Conductivity for Microscale Random Porous Media, *Phys. Rev. E*, 2007, **75**(3), p 10
17. R.W. Rice, Porosity Dependence of Physical Properties of Materials: A Summary Review, *Key Eng. Mater.*, 1996, **115**, p 1-19
18. J. Matejicek, B. Kolman, J. Dubsky, K. Neufuss, N. Hopkins, and J. Zwick, Alternative Methods for Determination of Composition and Porosity in Abradable Materials, *Mater. Charact.*, 2006, **57**(1), p 17-29
19. T. Mathews, G.P. Matthews, C.J. Ridgway, and A.K. Moss, Measurement of Void Size Correlation in Inhomogeneous Porous Media, *Transp. Porous Media*, 1997, **28**(2), p 135-158
20. D.G. Puerta, The Preparation and Evaluation of Thermal Spray Coatings: Mounting, *J. Therm. Spray Technol.*, 2005, **14**(4), p 450-452
21. D.G. Puerta, The Preparation and Evaluation of Thermal Spray Coatings: Grinding, *J. Therm. Spray Technol.*, 2006, **15**(1), p 31-32
22. D.G. Puerta and G. Blann, The Preparation and Evaluation of Thermal Spray Coatings: Fine Grinding and Polishing—Accepted Practices of Thermal Spray Technology, *J. Therm. Spray Technol.*, 2006, **15**(2), p 174-176
23. L. Kubinova, J. Janacek, J. Albrechtova, and P. Karen, Stereological and Digital Methods for Estimating Geometrical Characteristics of Biological Structures Using Confocal Microscopy, *From Cells to Proteins: Imaging Nature Across Dimensions*, V. Evangelista, L. Barsanti, V. Passarelli and P. Gualtieri, Ed., Springer, New York, 2005, p 271-321
24. K.A. Leithner, Basics of Quantitative Image Analysis, *Adv. Mater. Process.*, 1993, **141**(11), p 18-23
25. B. Ralph, L. Wojnar, K.J. Kurzydlowski, and J. Cwajna, 9th ECSIA and 7th STERMAT: Stereology and Image Analysis in Materials Science—Preface, *Mater. Charact.*, 2006, **56**(4-5), p 256
26. J. Michalski, T. Wejrzanowski, R. Pielaszek, K. Konopka, W. Lojkowski, and K.J. Kurzydlowski, Application of Image Analysis for Characterization of Powders, *Mater. Sci. (Poland)*, 2005, **23**(1), p 79-86

27. D. Shindo, Y. Ikematsu, S.H. Lim, and I. Yonenaga, Digital Electron Microscopy on Advanced Materials, *Mater. Charact.*, 2000, **44**(4-5), p 375-384
28. A.K. Datye, Electron Microscopy of Catalysts: Recent Achievements and Future Prospects, *J. Catal.*, 2003, **216**(1-2), p 144-154
29. P. Ctibor, R. Lechneroca, and V. Benes, Quantitative Analysis of Pores of Two Types in a Plasma-Sprayed Coating, *Mater. Charact.*, 2006, **56**(4-5), p 297-304
30. J. Ilavsky, G.G. Long, A.J. Allen, L. Leblanc, M. Prystay, and C. Moreau, Anisotropic Microstructure of Plasma-Sprayed Deposits, *J. Therm. Spray Technol.*, 1999, **8**(3), p 414-420
31. H. Nakahira, K. Tani, K. Miyajima, and Y. Harada, Anisotropy of Thermally Sprayed Coatings, *13th International Thermal Spray Conference—Thermal Spray: International Advances in Coatings Technology*, C.C. Berndt, Ed., May 28-June 5, 1992 (Orlando, FL), ASM International, Materials Park, OH, 1992, p 1011-1017
32. J. Ilavsky, A.J. Allen, G.G. Long, S. Krueger, H. Herman, C.C. Berndt, and A.N. Goland, Anisotropy of the Surfaces of Pores in Plasma Sprayed Alumina Deposits, *14th International Thermal Spray Conference: Thermal Spraying-Current Status and Future Trends*, A. Ohmori, Ed., High Temperature Society of Japan, 1993, p 483-488
33. P. Ctibor, P. Hofmann, P. Chraska, R. Lechnerova, and V. Benes, 3D Visualization of Thermally Sprayed Microstructure, *Thermal Spray 2007: Global Coating Solutions, International Thermal Spray Conference and Exposition*, 14-16 May, 2007 (Beijing, China), ASM International, Materials Park, OH, 2007, p 878-883
34. J.R. Wilson, W. Kobsiriphat, R. Mendoza, H.Y. Chen, J.M. Hiller, D.J. Miller, K. Thornton, P.W. Voorhees, S.B. Adler, and S.A. Barnett, Three-Dimensional Reconstruction of a Solid-Oxide Fuel-Cell Anode, *Nat. Mater.*, 2006, **5**(7), p 541-544
35. T. Allen, *Particle Size Measurement*, 5th ed., Chapman & Hall, New York, 1997
36. S.R. Stock, X-ray Microtomography of Materials, *Int. Mater. Rev.*, 1999, **44**(4), p 141-164
37. T. Narayanan, Synchrotron Small-Angle X-ray Scattering, *Soft Matter: Scattering, Imaging and Manipulation*, R. Borsali and R. Pecora, Ed., Springer, Berlin, 2007
38. J. Ilavsky, A.J. Allen, G.G. Long, and P.R. Jemian, Effective Pinhole-Collimated Ultrasmall-Angle X-Ray Scattering Instrument for Measuring Anisotropic Microstructures, *Rev. Sci. Instrum.*, 2002, **73**(3), p 1660-1662
39. A. Guinier and G. Fournet, *Small-Angle Scattering of X-rays*, John Wiley and Sons, New York, 1955
40. A.J. Allen, J. Ilavsky, G.G. Long, J.S. Wallace, C.C. Berndt, and H. Herman, Microstructural Characterization of Yttria-Stabilized Zirconia Plasma-Sprayed Deposits Using Multiple Small-Angle Neutron Scattering, *Acta Mater.*, 2001, **49**(9), p 1661-1675
41. J. Ilavsky, A. Allen, T. Dobbins, A. Kulkarni, and H. Herman, Microstructure Characterization of Thermal Barrier Coating Deposits—Practical Models from Measurements, *Thermal Spray Connects: Explore Its Surfacing Potential! Proceedings of the ITSC 2005*, E. Lugscheider, Ed., May 2-4, 2005 (Basel, Switzerland), ASM International, Materials Park, OH, p 516-524
42. A.F. Renteria, B. Saruhan, J. Ilavsky, and A.J. Allen, Application of USAXS Analysis and Non-interacting Approximation to Determine the Influence of Process Parameters and Ageing on the Thermal Conductivity of Electron-Beam Physical Vapor Deposited Thermal Barrier Coatings, *Surf. Coat. Technol.*, 2007, **201**(8), p 4781-4788
43. A.F. Renteria, B. Saruhan-Brings, and J. Ilavsky, Determination of the Relation Between the Process Controlled Variations of Anisotropic Void System and Thermal Conductivity of Electron Beam Physical Vapour Deposited (EB-PVD) PYSZ Thermal Barrier Coatings, *Ceram. Eng. Sci. Proc.*, 2007, **27**(3), p 3-16
44. T.A. Dobbins, A.J. Allen, J. Ilavsky, G.G. Long, P.R. Jemian, A. Kulkarni, and H. Herman, Recent Developments in the Characterization of Anisotropic Void Populations in Thermal Barrier Coatings Using Ultra-Small Angle X-Ray Scattering, *Ceram. Sci. Eng. Proc.*, 2003, **24**(3), p 517-524
45. T.J. Lu, C.G. Levi, H.N.G. Wadley, and A.G. Evans, Distributed Porosity as a Control Parameter for Oxide Thermal Barriers made by Physical Vapor Deposition, *J. Am. Ceram. Soc.*, 2001, **84**(12), p 2937-2946
46. J. Ilavsky, G.G. Long, A.J. Allen, H. Herman, and C.C. Berndt, The Effect of Spray Distance and Chemistry on Pore and Crack Development in Plasma Sprayed Ceramic Deposits, *9th National Thermal Spray Conference—Thermal Spray: Practical Solutions for Engineering Problems*, C.C. Berndt, Ed. (Cincinnati, OH), ASM International, Materials Park, OH, p 725-728
47. J. Ilavsky, G.G. Long, A.J. Allen, C.C. Berndt, and H. Herman, Changes in the Microstructure of Plasma-Sprayed Yttria-Stabilized Zirconia Deposits During Simulated Operating Conditions, *1st United Thermal Spray Conference—Thermal Spray: A United Forum for Scientific and Technological Advances*, C.C. Berndt, Ed., ASM International, Materials Park, OH, 1997, p 697-702
48. J. Ilavsky, A.J. Allen, G.G. Long, S. Krueger, C.C. Berndt, and H. Herman, Influence of Spray Angle on the Pore and Crack Microstructure of Plasma-Sprayed Deposits, *J. Am. Ceram. Soc.*, 1997, **80**(3), p 733-742
49. J. Ilavsky, B. Kolman, K. Neufuss, and P. Chraska, Influence of Spray Angle on the Microstructure of YSZ and Alumina Plasma-Sprayed Deposits, *2nd United Thermal Spray Conference,* E. Lugscheider and P.A. Kammer, Ed., March 17-19, 1999 (Düsseldorf, Germany), DVS Verlag, Düsseldorf, 1999, p 820-824
50. J. Ilavsky, A.J. Allen, G.G. Long, H. Herman, and C.C. Berndt, Characterization of the Closed Porosity in Plasma-Sprayed Alumina, *J. Mater. Sci.*, 1997, **32**(13), p 3407-3410
51. J. Ilavsky, H. Herman, C.C. Berndt, A.N. Goland, G.G. Long, S. Krueger, and A.J. Allen, Porosity in Plasma Sprayed Alumina Deposits, *6th National Thermal Spray Conference—Thermal Spray Industrial Applications*, C.C. Berndt and S. Sampath, Ed. (Boston, MA), ASM International, Materials Park, OH, 1994, p 709-714
52. A.J. Allen, G.G. Long, J. Wallace, J. Ilavsky, C.C. Berndt, and H. Herman, Microstructural Changes in YSZ Deposits During Annealing, *2nd United Thermal Spray Conference*, E. Lugscheider and P.A. Kammer, Ed., March 17-19, 1999 (Düsseldorf, Germany), DVS Verlag, Düsseldorf, 1999, p 228-233
53. A.J. Allen, N.F. Berk, J. Ilavsky, and G.G. Long, Multiple Small-Angle Neutron Scattering Studies of Anisotropic Materials, *Appl. Phys. A*, 2002, **74**, p S937-S939
54. A.J. Allen, G.G. Long, and J. Ilavsky, Quantitative Studies of the Three Void Systems in Plasma-Spray Deposits by Anisotropic Multiple Small-Angle Neutron Scattering, *MRS Fall Meeting '97—The Science and Technology of Thermal Spray Materials Processing, Materials Research Society*, December 1-5, 1997 (Boston, MA), Materials Research Society (MRS), Warrendale, PA, 1997, p 566
55. H. Boukari, A.J. Allen, G.G. Long, J. Ilavsky, J.S. Wallace, C.C. Berndt, and H. Herman, Small-Angle Neutron Scattering Study of the Role of Feedstock Particle Size on the Microstructural Behavior of Plasma-Sprayed Yttria-Stabilized Zirconia Deposits, *J. Mater. Res.*, 2003, **18**(3), p 624-634
56. T. Keller, W. Wagner, A. Allen, J. Ilavsky, N. Margadant, S. Siegmann, and G. Kostorz, Characterisation of Thermally Sprayed Metallic NiCrAlY Deposits by Multiple Small-Angle Scattering, *Appl. Phys. A*, 2002, **74**, p S975-S977
57. T. Keller, W. Wagner, J. Ilavsky, N. Margadant, S. Siegmann, J. Pisacka, G. Barbezat, J. Fiala, and T. Pirling, Microstructural Studies of Thermally Sprayed Deposits by Neutron Scattering, *Thermal Spray 2001—New Surfaces for a New Millennium*, C.C. Berndt, K.A. Khor, and E.F. Lugscheider, Ed., May 5-30, 2001 (Singapore), ASM International, Materials Park, OH, 2001, p 653-660
58. N. Margadant, S. Siegmann, J. Patscheider, T. Keller, W. Wagner, J. Ilavsky, J. Pisacka, G. Barbezat, P. Fiala, and T. Pirling, Microstructure-Property Relationships and Cross-Property-Correlations of Thermal Sprayed Ni-Alloy Coatings, *Thermal Spray 2001—New Surfaces for a New Millennium*, C.C. Berndt, K.A. Khor, and E.F. Lugscheider, Ed., May 5-30, 2001 (Singapore), ASM International, Materials Park, OH, 2001, p 643-665
59. J. Matejicek, J. Ilavsky, and T. Gnäupel-Herold, Neutron Scattering in Studies of Complex Anisotropic Microstructure,

Proceedings 3rd International Conference on Materials Structure and Micromechanics of Fracture, P. Sandera, Ed., June 27-29, 2001, Vutium, Brno, Czech Republic, 2001, p 502
60. A. Kulkarni, J. Gutleber, S. Sampath, A. Goland, W.B. Lindquist, H. Herman, A.J. Allen, and B. Dowd, Studies of the Microstructure and Properties of Dense Ceramic Coatings Produced by High-Velocity Oxygen-Fuel Combustion Spraying, *Mater. Sci. Eng. A*, 2004, **369**(1-2), p 124-137
61. A.A. Kulkarni, A. Goland, H. Herman, A.J. Allen, J. Ilavsky, G.G. Long, and F. De Carlo, Advanced Microstructural Characterization of Plasma-Sprayed Zirconia Coatings Over Extended Length Scales, *J. Therm. Spray Technol.*, 2005, **14**(2), p 239-250
62. P. Lu, J.J. Lannutti, P. Klobes, and K. Meyer, X-ray Computed Tomography and Mercury Porosimetry for Evaluation of Density Evolution and Porosity Distribution, *J. Am. Ceram. Soc.*, 2000, **83**(3), p 518-522
63. P. Vontobel, E.H. Lehmann, R. Hassanein, and G. Frei, Neutron Tomography: Method and Applications, *Physica B*, 2006, **385**, p 475-480
64. R.G. Cooper, SNS Detector Plans, *Nucl. Instrum. Methods Phys. Res. A*, 2004, **529**(1-3), p 394-398
65. R.D. Spal, Submicrometer Resolution Hard X-Ray Holography with the Asymmetric Bragg Diffraction Microscope, *Phys. Rev. Lett.*, 2001, **86**(14), p 3044-3047
66. M. Stampanoni, G. Borchert, and R. Abela, Progress in Microtomography with the Bragg Magnifier at SLS, *Radiat. Phys. Chem.*, 2006, **75**(11), p 1956-1961
67. M. Stampanoni, G. Borchert, and R. Abela, Towards Nanotomography with Asymmetrically Cut Crystals, *Nucl. Instrum. Methods Phys. Res. A*, 2005, **551**(1), p 119-124
68. A. Kulkarni, A. Goland, H. Herman, A.J. Allen, T. Dobbins, F. DeCarlo, J. Ilavsky, G.G. Long, S. Fang, and P. Lawton, Advanced Neutron and X-Ray Techniques for Insights into the Microstructure of EB-PVD Thermal Barrier Coatings, *Mater. Sci. Eng. A*, 2006, **426**(1-2), p 43-52
69. A. Kulkarni, Z. Wang, T. Nakamura, S. Sampath, A. Goland, H. Herman, J. Allen, J. Ilavsky, G. Long, J. Frahm, and R.W. Steinbrech, Comprehensive Microstructural Characterization and Predictive Property Modeling of Plasma-Sprayed Zirconia Coatings, *Acta Mater.*, 2003, **51**(9), p 2457-2475
70. A.A. Kulkarni, A. Goland, H. Herman, A.J. Allen, J. Ilavsky, G.G. Long, C.A. Johnson, and J.A. Ruud, Microstructure-Property Correlations in Industrial Thermal Barrier Coatings, *J. Am. Ceram. Soc.*, 2004, **87**(7), p 1294-1300
71. A.A. Kulkarni, H. Herman, J. Almer, U. Lienert, and D. Haeffner, Denth-Resolved Porosity Investigation of EB-PVD Thermal Barrier Coatings Using High-Energy X-Rays, *J. Am. Ceram. Soc.*, 2004, **87**(2), p 268-274
72. A.A. Kulkarni, S. Sampath, A. Goland, H. Herman, A.J. Allen, J. Ilavsky, W.Q. Gong, and S. Gopalan, Plasma Spray Coatings for Producing Next-Generation Supported Membranes, *Top. Catal.*, 2005, **32**(3-4), p 241-249
73. Z. Wang, A. Kulkarni, S. Deshpande, T. Nakamura, and H. Herman, Effects of Pores and Interfaces on Effective Properties of Plasma Sprayed Zirconia Coatings, *Acta Mater.*, 2003, **51**(18), p 5319-5334
74. S. Deshpande, A. Kulkarni, S. Sampath, and H. Herman, Application of Image Analysis for Characterization of Porosity in Thermal Spray Coatings and Correlation with Small Angle Neutron Scattering, *Surf. Coat. Technol.*, 2004, **187**(1), p 6-16
75. P. Fauchais, Suspension and Solution Plasma or HVOF Spraying, *J. Therm. Spray Technol.*, 2008, **17**(1), p 1-3
76. P. Fauchais, R. Etchart-Salas, V. Rat, J.F. Coudert, N. Caron, and K. Wittmann-Teneze, Parameters Controlling Liquid Plasma Spraying: Solutions, Sols, or Suspensions, *J. Therm. Spray Technol.*, 2008, **17**(1), p 31-59
77. K. Van Every, ''Development and Evaluation of Suspension Plasma Sprayed Yttria Stabilized Zirconia Coatings as Thermal Barriers,'' PhD Thesis, Purdue University, 2009
78. F. Azarmi, Vacuum Plasma Spraying, *Adv. Mater. Process.*, 2005, **163**(8), p 37-39
79. D.J. Nolan and M. Samandi, Revealing True Porosity in WC-Co Thermal Spray Coatings, *J. Therm. Spray Technol.*, 1997, **6**(4), p 422-424
80. J. Ilavsky, J. Pisacka, P. Chraska, N. Margadant, S. Siegmann, W. Wagner, P. Fiala, and G. Barbezat, Microstructure-Wear and Corrosion Relationships for Thermally Sprayed Metallic Deposits, *1st International Thermal Spray Conference—Thermal Spray: Surface Engineering via Applied Research*, C.C. Berndt, Ed., May 8-11, 2000 (Montréal, QC), ASM International, Materials Park, OH, 2000, p 449-454
81. J. Ilavsky, G.G. Long, A.J. Allen, and C.C. Berndt, Evolution of the Void Structure in Plasma-Sprayed YSZ Deposits During Heating, *Mater Sci. Eng. A*, 1999, **272**(1), p 215-221